

## VALIDATION OF OPEN SOURCE CFD APPLIED TO BUILDING EXTERNAL FLOWS

Rallou Dadioti<sup>1</sup>, Simon J. Rees<sup>2</sup>

<sup>1</sup>Institute of Energy and Sustainable Development, De Montfort University, Leicester, UK

<sup>2</sup>School of Civil Engineering, University of Leeds, LS1 9JT, UK

Email: [rallou.dadioti@gmail.com](mailto:rallou.dadioti@gmail.com)

### ABSTRACT

This paper examines the performance of conventional eddy viscosity and Detached Eddy Simulation (DES) turbulence models implemented in the open source CFD library OpenFOAM. For these purposes we revisit a number of benchmark data sets developed by the Architectural Institute of Japan. We firstly present results for analysis of the flow around a single high rise building and make comparisons with wind tunnel data. Secondly we examine predicted flows in a real urban environment. We find that the eddy viscosity models perform similarly to implementation in other CFD codes. Such modelling approaches give unsatisfactory performance in certain wind conditions, however. The DES results show better prediction of wind flows in comparison to both wind tunnel and field data in many cases.

### INTRODUCTION

#### **Background**

Calculation of external flows in complex urban environments using CFD methods is of value to studies of structural loads, pedestrian comfort, natural ventilation, contaminant dispersion and wind energy (Meroney et al., 2001; Blocken et al., 2012; Hooff and Blocken, 2010; Vardoulakis et al., 2003; Tabrizi et al., 2014). Despite the fact that the Large Eddy Simulation (LES) modelling approach is known to behave better than the Reynolds-Averaged Navier-Stokes (RANS) approaches using eddy-viscosity turbulence models, it is still expensive (often prohibitively so) in analysis of practical building external flows. A promising hybrid RANS/LES approach is Detached Eddy Simulation (DES) that treats boundary layer regions using a RANS model and transitions to LES mode in regions of separated flow.

#### **Aims and objectives**

The aim of this study is to offer some validation evidence for OpenFOAM software (Weller et al., 1998) applied to external flows in urban environments with commonly used eddy viscosity and DES turbulence models. Our further aim is to evaluate the advantages of DES approaches in these applications as this has been reported in very few papers. This work has been carried out in the context of study and development of CFD based methods for wind energy assessment in

complex urban environments. Hence we comment on modelling of wake conditions rather than evaluation of surface pressures and forces or dispersion of contaminants.

For these purposes we examine the performance of both steady RANS models as well as Delayed Detached Eddy Simulation approaches implemented in OpenFOAM using benchmark data derived from wind tunnel data as well as data derived from field measurements developed by the Architectural Institute of Japan (AIJ) (AIJ, 2009; Yoshie et al., 2007). A number of studies have previously been reported that make use of these test cases Tominaga et al. (2004).

#### **Application of OpenFOAM**

In this work we apply numerical models implemented in the OpenFOAM CFD library (Weller et al., 1998). OpenFOAM is a free, open-source CFD software library, that makes use of the object oriented features of the C++ programming language (Jasak et al., 2007). OpenFOAM has gradually gained popularity in both commercial and academic organisations, the reward of being free of charge, easily modifiable, adequate for a broad range of fluid dynamics applications, providing efficient parallel computing capabilities and the possibility to easily implement customised solvers and functions (Ghione, 2012). However, development of independent quality assurance data and documentation relies on the efforts of third parties. Some validation exercises where OpenFOAM models have been applied to wind flows have been published Balogh et al. (2012); Churchfield and Moriarty (2010); Flores et al. (2014) but these have not been concerned with urban environments.

In applying the first of the AIJ test cases we have used the steady-state RANS solver `simpleFoam` from the OpenFOAM library (version 2.3.1) with the standard  $k-\epsilon$ ,  $k-\omega$ -SST and Realizable  $k-\epsilon$  eddy viscosity turbulence models (Launder and Spalding, 1974; Menter, 1994; Shih et al., 1995). In the second test case involving a model of a real urban environment, we have applied the standard  $k-\epsilon$  model for the RANS calculations. The DES concept was developed by Spalart et al. (1997) for aerospace applications involving boundary layer separation. The DES model we have applied in both test cases is the DDES-SA model (Spalart et al., 2006) with the `pisofFoam` tran-

sient solver. This version of the Spalart-Allmaras DES model has some improvements over the original model (Spalart et al., 1997). These development seek to improve prediction of boundary layer separation points on aerofoils. This is not a particular issue in building external flows as separation is generally forced by reverse right-angle features at roof and wall edges rather than curved surfaces.

The main advantage of DES approaches in the case of urban wind flows is that coarser grids and larger time-steps can be taken than would otherwise be required for true LES. We see the ability to capture the features of wake regions by calculations in LES mode to be the most significant advantage in these types of problem as buildings in dense urban environments are generally in the wake of neighbouring buildings rather than clean atmospheric boundary layer conditions.

### TEST CASE A: HIGH RISE BUILDING

#### General description of the experiment

The first test case is a study of the flowfield around a high-rise building of 2:1:1 (height:width:depth) ratio, placed in a turbulent boundary layer (Figure 1). The wind tunnel scale model was 0.16 m high and 0.08 m square. The wind tunnel imposed an inlet condition approximating a power law velocity profile with an exponent of around 0.27 and the Reynolds number was  $2.4 \times 10^4$  (Figure 1).

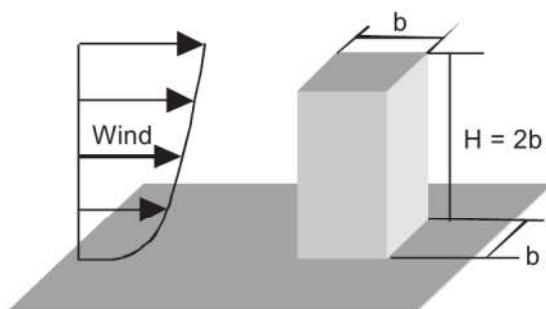


Figure 1: 2:1:1 shaped building geometry.  $b=0.08m$ . The velocity profile is  $U = z^{0.27}$  (Yoshie et al., 2007). The roof and rear reattachment lengths are defined as  $X_R$  and  $X_F$  respectively

Measurements were taken using a split-film probe for the instantaneous wind velocity in each direction and the average and standard deviation of fluctuating wind velocities were reported (Yoshie et al., 2007). Measurements of the velocities were made at a grid of points over a vertical cross-section and on horizontal

planes as indicated in Figure 2. The data used in our first validation study is that published by Meng and Hibi (1998).

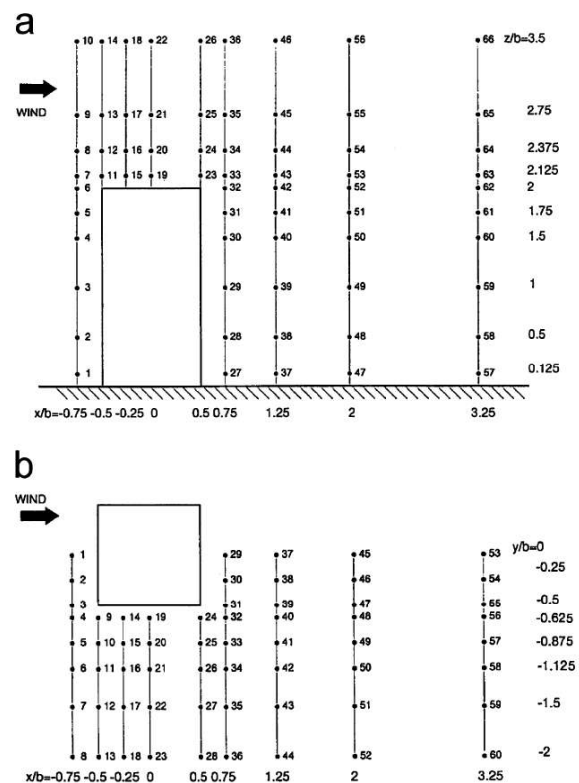


Figure 2: The Test Case A wind tunnel experiment. (a) Measuring points in vertical cross-section ( $y = 0$ ). (b) Measuring points in horizontal plane ( $z = 0.125b$  and  $1.25b$ ) (Yoshie et al., 2007).

#### Computational domain and mesh

The dimensions of the computational domain are  $L \times W \times H = 21b \times 13.75b \times 11.25b$  (with  $b$  being the width of the building) and replicate the geometry of the wind tunnel—as recommended in best practice guidelines Franke et al., 2007. The experiment parameters have been reported by Tominaga et al., 2008 and are the standard conditions for the comparative studies with the wind tunnel data as well as the CFD results of other working groups.

The mesh resolution for the RANS calculations was  $60(x) \times 45(y) \times 39(z)$  (105,300 cells) and the building was discretized into  $10 \times 10 \times 16$ . The minimum grid width is set to  $0.07b$  and is expanded towards the horizontal and the vertical directions. This follows similar practice to other CFD studies of this case reported by Tominaga et al., 2008. A finer mesh was used for the DES calculations and contained approximately 1.1 million cells. Figure 3 illustrates these mesh arrangements.

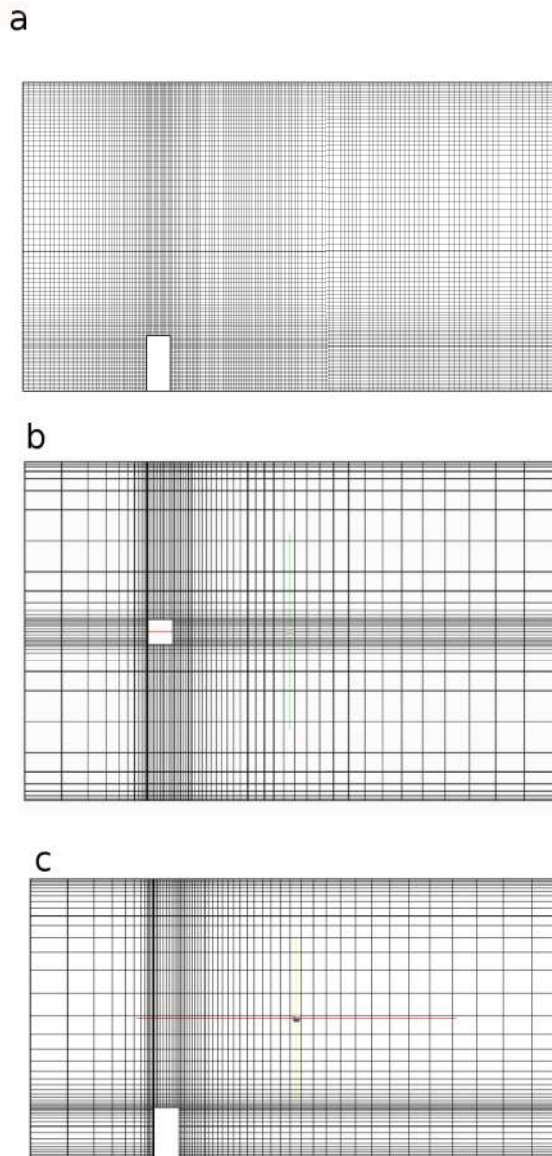


Figure 3: Test case A grid discretization for: (a) DES cases; (b, c) RANS cases.

### Boundary Conditions

The conditions shown in Table 1 are the standard boundary conditions for the RANS calculations—following the practices reported by Yoshie et al., 2007. Symmetry conditions were applied at the lateral and upper surfaces in the DES calculations.

## TEST CASE B: ACTUAL URBAN AREA

### General description of the experiment

The second test case is a study of the flow field within a building complex in the Shinjuku sub-central area of Tokyo, Japan (Figure 4). A number of wind tunnel experiments as well as field measurements were carried out by various research institutions around the time of construction. In this and other reported studies

the CFD simulations were performed for conditions recorded in 1977 (Yoshie et al., 2007). The case is of particular interest as it has a complex geometry with large variation in building heights. The data set has additional value as it includes field measurements as well as wind tunnel test data. In the field tests three cup anemometers were used, taking measurements at 10 m height from the ground for the points 1 to 36 and at 192 m and 242 m for the C and D points shown in Figure 5.

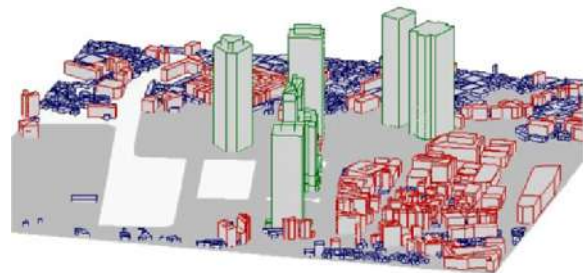


Figure 4: Building complexes in urban area of Shinjuku (Yoshie et al., 2007) that define the geometry of Test Case B.

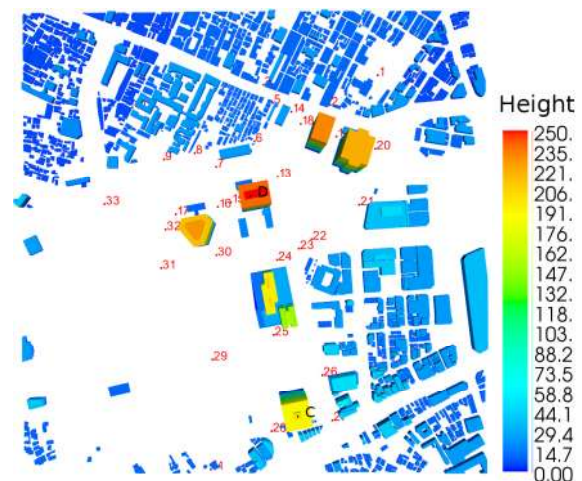


Figure 5: Test case B measuring points and building heights (Shinjuku)

### Computational domain and mesh

The computational domain is firstly defined by CAD data representing  $1000 \times 1000$  m of the Shinjuku sub-central area (Figure 5). This building geometric data extends for approximately one block beyond the central region containing the measurement points (the exception being point 11 close to the south border) and this follows the AIJ guidance (Yoshie et al., 2007). The dimensions of the complete domain are  $L \times W \times H = 5742 \times 3372 \times 1422$  m<sup>3</sup> accommodating an upstream length of  $5H$  (with  $H$  being the height of the highest building), a downstream subdomain length of  $15H$  and a height of  $6H$ . The lateral boundaries have been placed  $5H$  from the Shinjuku partition in accordance with best practice guidelines (Franke et al., 2007; Tominaga et al., 2008).

Table 1: Standard Boundary Conditions (Yoshie et al., 2007)

Inflow	Interpolated values of U and k from the experimental flow
Outflow	Zero gradient
Lateral and upper surfaces of the domain	Logarithmic law for a smooth wall
Ground surface	Logarithmic law with roughness length $z_0$ ( $z_0 = 1.8 \times 10^4$ m)
Building surface	Logarithmic law for a smooth wall

This case study has geometric complexity representative of urban environments of practical interest and represents a challenge in terms of mesh generation. The OpenFOAM snappyHexMesh tool has proved able to mesh the case study geometry with a high degree of automation and good parallel efficiency. The tool generates hex-dominant meshes with an octree topology whereby a background cubic mesh is subdivided a number of times as the ground and building surfaces are approached. At the building surfaces the cells are modified to snap to the underlying CAD geometry (triangulated Stereolithography format in this case).

Parts of the computational grid are presented in Figure 6 to demonstrate the refinement regions around the buildings. The total number of cells for the whole domain was approximately 11.5 million for the west wind direction illustrated. Similar results were obtained by simply rotating the background mesh to obtain meshes for the other wind directions resulting in meshes with comparable numbers of cells. Boundary conditions were treated in a similar manner to Test Case A.

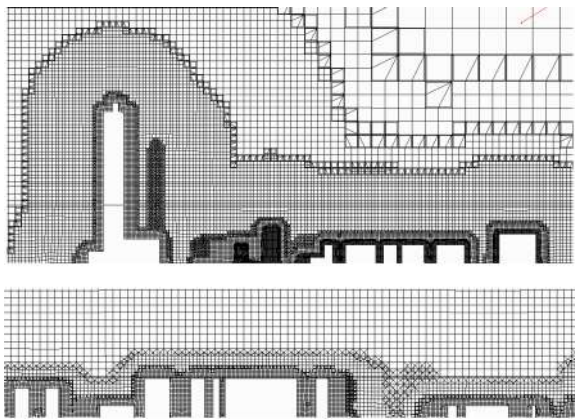


Figure 6: Parts of the computational grid

## RESULTS

### Test Case A results

Experimental data for Test Case A, and results of other related CFD studies, are available in the form of predictions of reattachment lengths ( $X_F$  and  $X_R$  in Figure 1) and mean velocities at a the grid of points shown in Figure 2. A synopsis of the computed reattachment lengths are presented in Table 2. These are the CFD results for the RANS simulations utilizing different turbulence models and the hybrid DDES-SA model

with reattachment lengths estimated from examining the mean longitudinal wind velocities near the roof and ground surfaces.

Table 2: Test Case A Results: Computed reattachment lengths.

#	CFD model	Turbulence model	$x_F/b$	$x_R/b$
1	RANS	Standard k- $\epsilon$	2.68	0.50
2	RANS	Realizable k- $\epsilon$	5.37	0.50
3	RANS	k- $\omega$ -SST	2.59	0.30
4	LES/RANS	DDES-SA	2.39	0.38
5	Experiment		1.42	0.52

In all cases the rear reattachment lengths are over predicted with the prediction of the DDES-SA calculation being closest to the experimental value. Tominaga et al. (2004) presented 11 sets of results for this test case and also found  $X_F/b$  was over predicted (a range of 1.98-2.7 for different implementations of the standard k- $\epsilon$  model). Lower values closer to the experimental result were only found using LES or DNS approaches in that study. The behaviour in the wake is further illustrated in Figure 8. This shows similar features in the standard k- $\epsilon$  and DDES-SA flow near the reattachment point. However, there are further differences further downstream as the flow returns towards its undisturbed condition—unfortunately no wind tunnel measurements are available for this region and so we can't comment further.

The recirculation zone near the leading edge of the roof and the associated reattachment length ( $x_R$  in Figure 1), which was observed in the wind tunnel experiments, was only reproduced in the RANS calculations with the k- $\omega$ -SST turbulence model (Table 2). The DDES-SA and other RANS results show the flow attached over part of the the roof but no clear reversal of flow. Similar variability in the prediction of this feature was noted by Tominaga et al. (2004).

Figure 7 presents the distribution of the mean horizontal velocity ( $\bar{U}_x$ ) on a vertical mid plane ( $y = 0$ ) and on two horizontal planes. One horizontal plane is near the ground ( $z = 0.125b$ ) and one part way up the building ( $z = 1.25b$ ). The positions of the measuring lines are illustrated with the dotted lines which also represent the origin for the calculated wind velocities i.e. positive values are plotted on the right side of the line, and negative values on the left side (Yoshie et al., 2007).

In general, where the mean velocities are compared at the measurement points (Figure 7) there is good cor-

rependance between the CFD results and the wind tunnel data. The main differences in these velocity profiles are found near the building surfaces and the edges of the wake i.e. at locations of higher velocity gradient or rate of shear. The DDES-SA results and Standard  $k-\epsilon$  turbulence model results generally show best agreement with the experimental data. In the horizontal plane part way up the building ( $z = 1.25b$ ) horizontal velocities are noticeably underestimated inside the wake region. In the horizontal plane near the ground surface ( $z = 0.125b$ ) the DDES-SA results are noticeably better than all the RANS models.

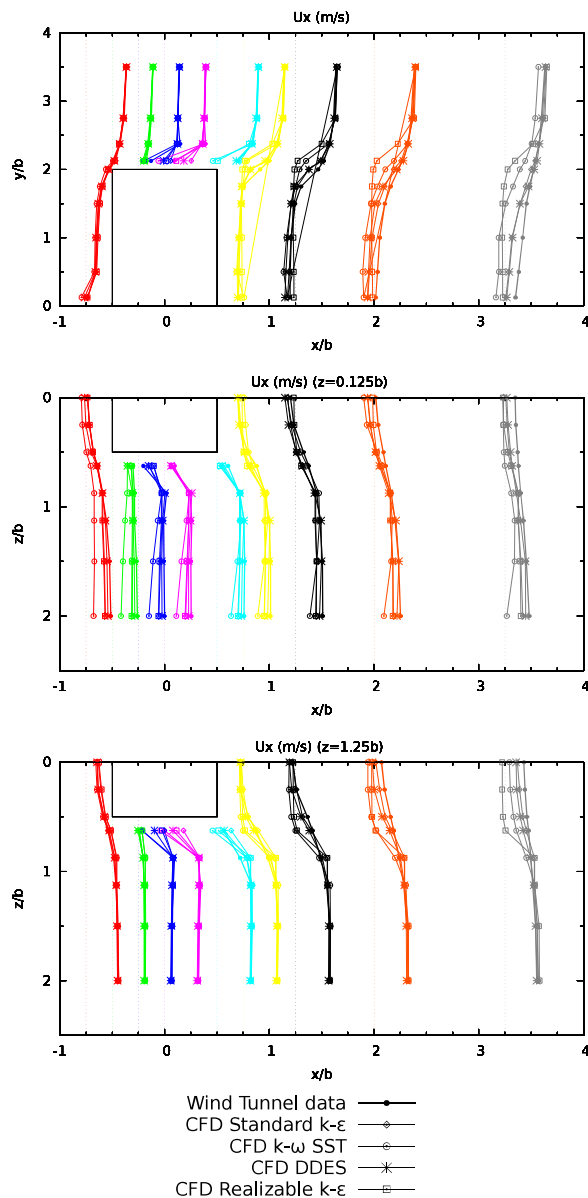


Figure 7: Distribution of  $\bar{U}_x$  in a vertical plane on the centreline (a) and in horizontal planes at heights  $0.125b$  and  $1.25b$ .

Visualisation of the instantaneous velocities calculated with the DDES-SA model have given some insight into the behaviour in the wake region. The aspect ratio of the building means that the eddy structures gener-

ated by the vertical leading edges dominate those generated at the leading edge of the roof. The largest eddy structures flowing from the roof are transported over the eddy structures near the ground at the leeward side of the building. The flow in the wake region accordingly seems more complex, with stronger mixing, than flows over cubes. This has also been pointed out by Tominaga et al. (2004). It appears that consequently there are periods in the vortex shedding cycle where the wake is extended and the reattachment point is very mobile. This gives some clue as to why it was difficult to achieve convergence with the Realizable model. This is to be investigated further.

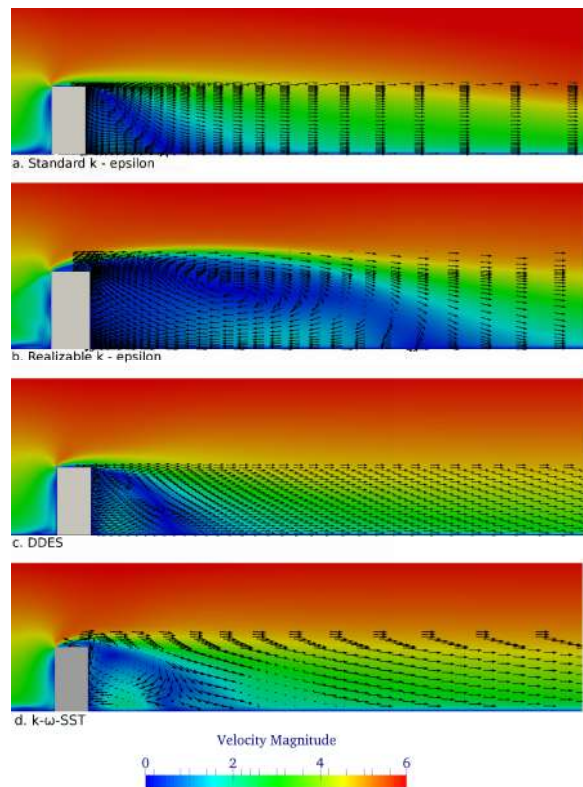


Figure 8: Velocity vectors and magnitude data on a vertical plane through the centre of the wake region.

### Test Case B results

To compare the CFD results with the field measurements and the wind tunnel data the computational wind speed has been normalised by the wind speed at reference point D (the top of the Shinjuku Mitsui Building) at a height of 242 m for the north wind direction and point C (the top of the KDD Building) at 192 m height for the other wind directions as in previous studies.

Figure 9 presents the calculated wind speed ratios alongside the field measurements and the wind tunnel data (where available), at the measuring points for four wind directions (East, South, West and North). In 44 of the total of 60 comparisons, results for the DDES-SA model fall within one standard deviation of the field measurements and only 5 fall significantly outside this band. The RANS results fall outside the

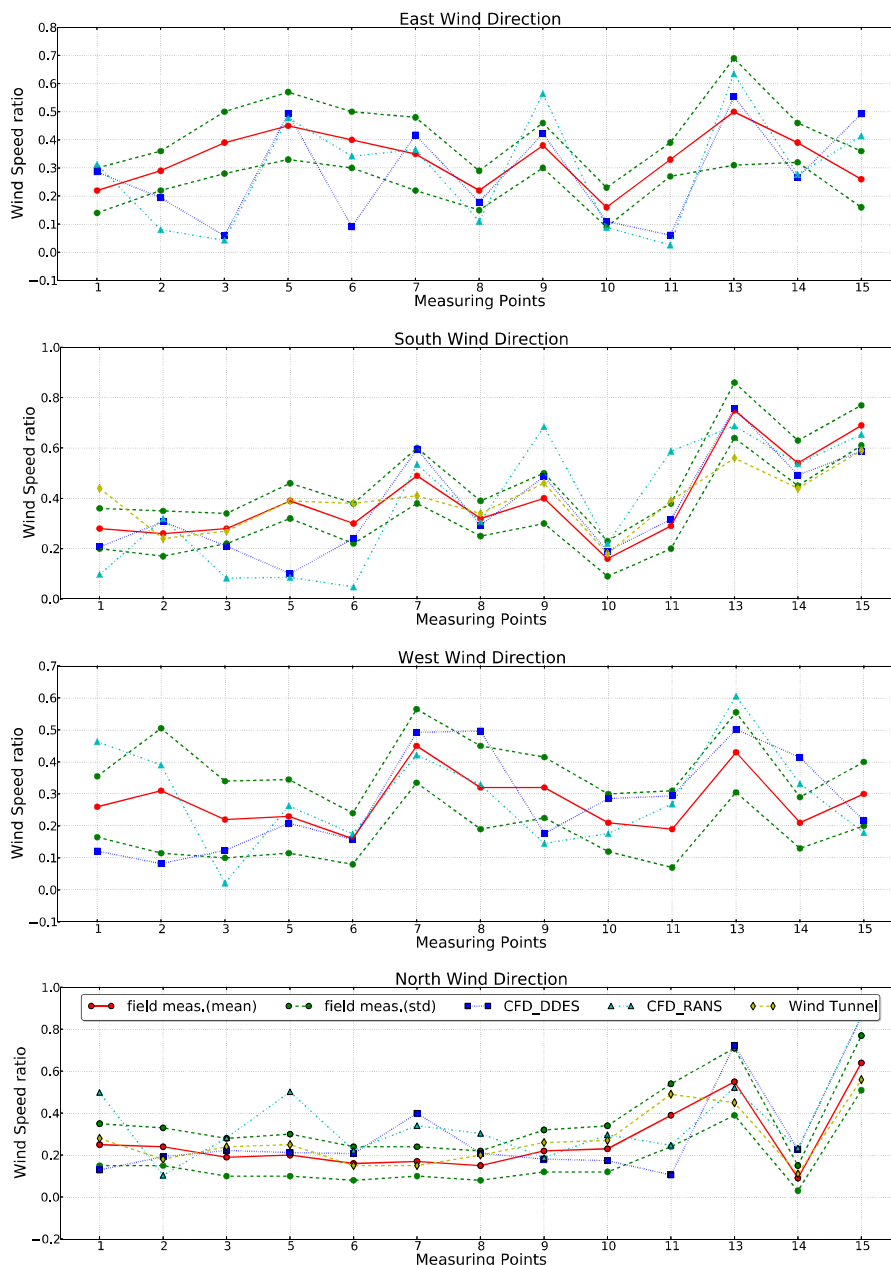


Figure 9: Comparison of predicted and measured wind speed ratios at the reference measuring points. The North and South wind directions include field study data.

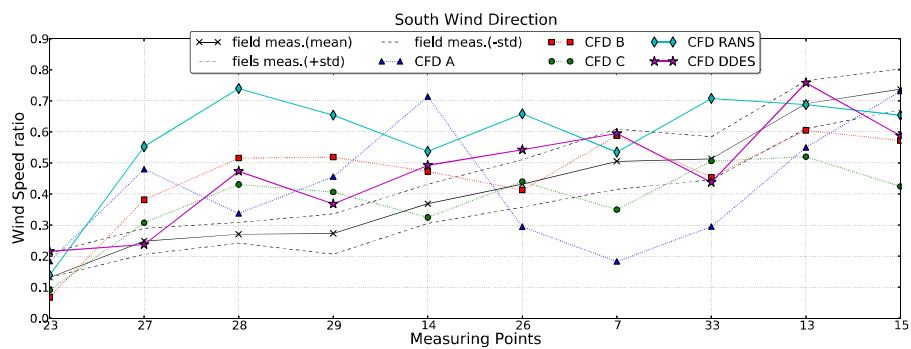


Figure 10: Comparison of wind speed ratio at reference Points measuring points with wind direction South.

one standard deviation band in 24 out of a total of 60 tests—12 are significantly outside.

The superior performance of the DDES-SA model is also demonstrated in **Figure 10**, where the results are compared with the RANS results for other CFD codes published by a working group of the Architectural Institute of Japan **Tominaga et al., 2005**. In this figure the measurement points are shown in order of increasing mean velocity.

A qualitative review of the results (**Figure 11**) shows that the complex flow patterns of the interaction between the wind flow and building is well reproduced by the DDES-SA calculations, including such details as the horseshoe vortex shape (h1, h2 and h3 regions) and the reattachment zones behind the buildings (r1, r2 and r3 regions). In the RANS results (**Figure 11** right) these vortices are not as well defined and the size of the recirculation zone in the wake of the buildings is overestimated.

## CONCLUSIONS

In this work we investigated the prediction capabilities of numerical models implemented using the OpenFOAM CFD library and revisiting two test cases developed by the Architectural Institute of Japan that provide benchmark data derived from wind tunnel testing and field measurements. We examined the performance of both steady-state RANS approaches with some eddy-viscosity turbulence models as well as a hybrid RANS/LES approach with the Delayed Detached Eddy Simulation (DDES-SA) turbulence model. The test cases represent an idealized building with 2:1:1 aspect ratios and a real urban geometry with considerable geometric complexity. The tests have examined mean velocity predictions and boundary layer reattachment lengths.

Calculations of wind flows around buildings using RANS approaches and two-equation turbulence models are known to have limitations, particularly in calculating conditions in wake regions. We found this to be the case with the models of this type we evaluated using OpenFOAM and that predictions were comparable with what has been published in earlier studies for these types of model. Results from applying DES approaches to these test cases has not been published before. Results we obtained with the DDES-SA model have been noticeably better than those from the RANS models, particularly in wake regions where LES is the mode of calculation although not in all cases. We conclude that this approach, although significantly more computationally demanding than RANS calculations, offers improved robustness and accuracy over a range of wind conditions. Accordingly, we intend to pursue the application of DES approaches using OpenFOAM in the further study of wind flows at the campus where we are collecting high frequency anemometer data for further validation exercises.

## REFERENCES

- AIJ 2009. Guidebook for Practical Application of CFD to Pedestrian Wind Environment around Buildings. Available online [accessed 12/5/15] <http://www.aij.or.jp/jpn/publish/cfdguide>.
- Balogh, M., Parente, a., and Benocci, C. 2012. RANS simulation of ABL flow over complex terrains applying an Enhanced k- $\epsilon$  model and wall function formulation: Implementation and comparison for fluent and OpenFOAM. *Journal of Wind Engineering and Industrial Aerodynamics*, 104-106:360–368.
- Blocken, B., Janssen, W., and van Hooff, T. 2012. CFD simulation for pedestrian wind comfort and wind safety in urban areas: General decision framework and case study for the Eindhoven University campus. *Environmental Modelling and Software*, 30:15–34.
- Churchfield, M. J. and Moriarty, P. J. 2010. Wind Energy-Related Atmospheric Boundary Layer Large-Eddy Simulation Using OpenFOAM. In *19th Symposium on Boundary Layers and Turbulence*, Keystone, Colorado.
- Flores, F., Garreaud, R., and Muñoz, R. C. 2014. OpenFOAM applied to the CFD simulation of turbulent buoyant atmospheric flows and pollutant dispersion inside large open pit mines under intense insolation. *Computers & Fluids*, 90:72–87.
- Franke, J., Hellsten, A., Schlünzen, H., and Carissimo, B. 2007. *Best practice guideline for the CFD simulation of flows in the urban environment*, COST Action 732. European Science Foundation COST Office.
- Ghione, A. 2012. Development and validation of a two-phase cfd model using openfoam. Master's thesis, KTH, Stockholm.
- Hooff, T. V. and Blocken, B. 2010. On the effect of wind direction and urban surroundings on natural ventilation of a large semi-enclosed stadium. *Computers & Fluids*, 39(7):1146–1155.
- Jasak, H., Tukovic, Z., and Jemcov, A. 2007. OpenFOAM: A C++ Library for Complex Physics Simulations. In *International Workshop on Coupled Methods in Numerical Dynamics*, volume m, pages 1–20, Dubrovnik, Croatia.
- Launder, B. and Spalding, D. 1974. The numerical computation of turbulent flows.
- Meng, Y. and Hibi, K. 1998. Cooperative project for CFD prediction of pedestrian wind environment in the architectural institute of japan. *Journal of Wind Engineering, Japan*, 76:55–64.

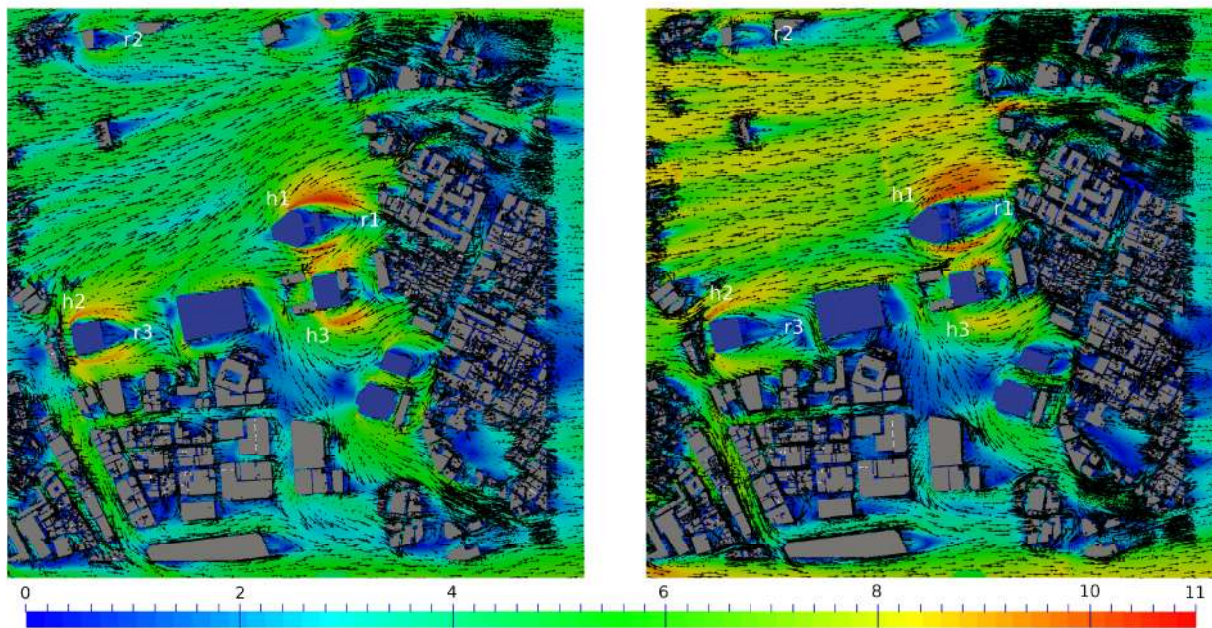


Figure 11: Vectors of the wind velocity at a plane 10 m above the ground for the DDES-SA model (left) and the RANS model (right).

Menter, F. R. 1994. Two-equation eddy-viscosity turbulence models for engineering applications.

Meroney, R. N., d Neff, D. E., Chang, C.-h., and Pradoto, R. 2001. Computational Fluid Dynamics and Physical Model Comparisons of Wind Loads and Pedestrian Comfort Around a High Rise Building. In *Inaugural Meeting of Wind Engineering Research Center, Tokyo Institute of Polytechnics, (TIP), Atsugi, Japan, October 20.*, page 2.

Shih, T.-H., Liou, W. W., Shabbir, A., Yang, Z., and Zhu, J. 1995. A new k- eddy viscosity model for high reynolds number turbulent flows - model development and validation. *Computers & Fluids*, 24(3):227–238.

Spalart, P. R., Deck, S., Shur, M. L., Squires, K. D., Strelets, M. K., and Travin, A. 2006. A New Version of Detached-eddy Simulation, Resistant to Ambiguous Grid Densities. *Theoretical and Computational Fluid Dynamics*, 20(3):181–195.

Spalart, P. R., Jou, W. H., Strelets, M., and Allmaras, S. R. 1997. Comments on the feasibility of LES for wings and on a hybrid RANS/LES approach.

Tabrizi, A. B., Whale, J., Lyons, T., and Urmee, T. 2014. Performance and safety of rooftop wind turbines: Use of CFD to gain insight into inflow conditions. *Renewable Energy*, 67:242–251.

Tominaga, Y., Mochida, A., Shirasawa, T., Yoshie, R., Kataoka, H., Harimoto, K., and Nozu, T. 2004. Cross Comparisons of CFD Results of Wind Environment at Pedestrian Level around a High-rise

Building and within a Building Complex. *Journal of Asian Architecture and Building Engineering*, 3(1):63–70.

Tominaga, Y., Mochida, A., Yoshie, R., Kataoka, H., Nozu, T., Yoshikawa, M., and Shirasawa, T. 2008. AIJ guidelines for practical applications of CFD to pedestrian wind environment around buildings. *Journal of Wind Engineering and Industrial Aerodynamics*, 96(10):1749 – 1761.

Tominaga, Y., Yoshie, R., Mochida, A., Kataoka, H., Harimoto, K., and Nozu, T. 2005. Cross comparisons of CFD prediction for wind environment at pedestrian level around buildings. comparison of results for flowfield around building complex in actual urban area. In *The Sixth Asia-Pacific Conference on Wind Engineering (APCWE-VI) Seoul, Korea*.

Vardoulakis, S., Fisher, B. E., Pericleous, K., and Gonzalez-Flesca, N. 2003. Modelling air quality in street canyons: a review. *Atmospheric environment*, 37(2):155–182.

Weller, H. G., Jasak, H., and Tabor, G. 1998. A tensorial approach to computational continuum mechanics using object-oriented techniques. *Computers in Physics*, 12(6):620–631.

Yoshie, R., Mochida, A., Tominaga, Y., Kataoka, H., Harimoto, K., Nozu, T., and Shirasawa, T. 2007. Cooperative project for CFD prediction of pedestrian wind environment in the architectural institute of japan. *Journal of Wind Engineering and Industrial Aerodynamics*, 95(911):1551 – 1578.